ELSEVIER

Physica D 157 (2001) 197–206

PHYSICA D

www.elsevier.com/locate/physd

How tangled is a tangle?

Carlo F. Barenghi [a,*], Renzo L. Ricca [a,1], David C. Samuels [b]

[a] *Isaac Newton Institute for Mathematical Sciences, University of Cambridge, Cambridge CB3 0EH, UK*
[b] *Mathematics Department, University of Newcastle, Newcastle NE1 7RU, UK*

Received 11 December 2000; received in revised form 24 May 2001; accepted 1 June 2001
Communicated by U. Frisch

Abstract

New measures of algebraic, geometric and topological complexity are introduced and tested to quantify morphological aspects of a generic tangle of filaments. The tangle is produced by standard numerical simulation of superfluid helium turbulence, which we use as a benchmark for numerical investigation of complex systems. We find that the measures used, based on crossing number information, are good indicators of generic behaviour and detect accurately a tangle's complexity. Direct measurements of kinetic helicity are found to be in agreement with the other complexity-based measures, proving that helicity is also a good indicator of structural complexity. We find that complexity-based measure growth rates are consistently similar to one another. The growth rate of kinetic helicity is found to be twice that of energy.

PACS: 2.40; 5.45 Pq; 47.27; 67.40 Vs

Keywords: Tangle; Vortex; Complexity; Turbulence; Helicity; Superfluidity

1. Modelling complex tangles by superfluid vortices

Complex systems of filaments are ubiquitous in nature and arise in such disparate contexts as superfluid physics [1,2], plasma physics [3], polymer physics [4], molecular biology [5] and cosmic string theory [6]. It is important to be able to identify and analyse the morphological complexity of such systems and possibly develop relationships between complexity and energy. The aim of this paper is to introduce and test measures to address these two issues.

Recently theoretical progress has been made thanks to concepts and techniques borrowed from knot theory to study fluid flows and magnetic structures [7–10]. There is now a call for more work to be done to test these ideas and develop these concepts further. Information based on structural complexity may in fact play an important role in estimates of energy of physical systems. In the case of a magnetised fluid, where magnetic knots and links are present, the ground state magnetic energy $E_{\min}$ of the system is bounded from below by relationships of the type $E_{\min} \geq f(V, \Phi; N, c_{\min})$, where f is some functional relationship between total magnetic volume V, total magnetic flux Φ, number N of magnetic knots and topological crossing number $c_{\min}$ (see [11–13]). Ideally one would like to have expressions for the energy of the system in the form $E = f(V, \Phi; \mathcal{X})$, where

* Corresponding author. Permanent address: Mathematics Department, University of Newcastle, Newcastle NE1 7RU, UK.
E-mail address: c.f.barenghi@newcastle.ac.uk (C.F. Barenghi).
[1] Permanent address: Mathematics Department, University College London, London WC1E 6BT, UK.

0167-2789/01/$ – see front matter
PII: S0167-2789(01)00304-9

$\mathcal{X}$ is some measure of structural complexity of the system.

The aim of this paper is to test measures of algebraic, geometric and topological complexity and quantify morphological aspects of a generic tangle of vortex filaments and compare these quantities with measures of energy and helicity. The vortex tangle is produced by numerical simulation of superfluid helium turbulence, following a standard procedure. It has long been observed that above some small critical speed, helium II enters a dissipative, chaotic state, called superfluid turbulence [14,15]. We know that this state consists of a self-sustaining, apparently random tangle of highly localised inviscid superfluid vortex filaments. Unlike classical turbulence, in which each eddy can be of any size and strength, superfluid vortex filaments have all the same circulation $\Gamma = 9.97 \times 10^{-4}\,\mathrm{cm}^2/\mathrm{s}$ (the ratio of Plank's constant and the mass of helium) and the same vortex core radius $a_0 \approx 10^{-8}\,\mathrm{cm}$. Each filament moves under the effect of its local curvature (see Section 2 below), while advection is governed by mutual induction due to the surrounding filaments, and dissipation by the effect of friction against the normal (viscous) fluid. When two vortex filaments come sufficiently close to each other they reconnect [16] and the newly formed filaments move in a direction orthogonal to the original configuration plane (Fig. 1). Vortex reconnections thus provide a natural mechanism for randomising the morphology of the system, mimicking re-combination processes present in other contexts, such as polymer physics and molecular biology. Superfluid turbulence simulations provide therefore a convenient (and economical) numerical benchmark to investigate issues related to structural complexity of physical systems.

Superfluid turbulence is currently studied in the laboratory by moving liquid helium along channels and pipes using towed or oscillating grids, and by stirring the liquid using propellers [17–20]. The main quantity monitored and measured in these experiments is the total length of the vortex filaments, and this quantity is consistently reported in numerical investigations [21,22]. It is therefore important, for a comparison and for energy estimates, to keep track of the total length of the tangle during evolution. However, if we want to characterise structural and topological complexity we need to go further, in particular beyond metric information. Algebraic and topological measures of knottedness and linking, for example, provide useful information that do not depend on metric properties. Because of reconnections, a tangle's topology keeps changing, but it is possible that in a turbulent steady-state, in which average properties fluctuate around mean values, topological complexity provides also an alternative measure of average quantities. Geometric and topological properties can also be investigated during the growth and decay phase of the vortex tangle, and changes in morphology and topology can be usefully compared to the growth rates of physically important quantities such as kinetic energy and helicity.

In this paper, we concentrate on the phenomenon of growth of superfluid turbulence generated by the Glaberson instability [23,24], due to a super-imposed *ABC*-type of flow. The *ABC* flow, being highly helical, is very efficient to induce helicity and topological linking. The instability arises when the amplitude

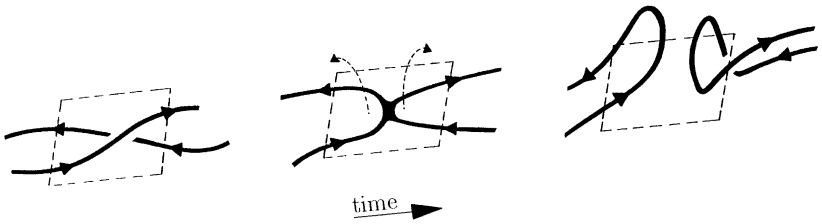

Fig. 1. A diagram of a typical reconnection process: when two vortex lines come sufficiently close to each other they reconnect and the newly formed filaments move in a direction orthogonal to the original configuration plane. Note that, during the process the orientation of the strands, induced by the prescribed vorticity and indicated by the arrows, is preserved.

of the component of the normal fluid velocity in the direction parallel to a superfluid vortex line exceeds a critical value. In this case, helical disturbances of the vortex lines become unstable and grow exponentially in amplitude. Large amplitude waves on nearby vortex lines interact and trigger reconnections, so that as in a cascade process the entire vortex structure becomes destabilised to form a complex vortex tangle. Previous investigations [23,24] show that vortex lines so produced tend in the long term to concentrate in bundles and form structures that mimic, in a coarse, grained sense, the vorticity distribution present in the normal fluid. Here we are not interested in the saturation process, that eventually stops the further growth of the tangle, but only in the phase of growth from interacting seed vortex rings till the formation of a mature tangle. Our aim is to compare the growth rate of measures of tangle's complexity against the known growth rate of length and energy.

2. Vortex dynamics and complexity measures

Following Schwarz [1,2], let us consider vortex lines in an unbounded fluid domain. A vortex line is represented by a three-dimensional closed curve $\mathcal{L}$ given by the vector equation $\mathbf{X} = \mathbf{X}(s,t)$, where s denotes arc-length and t time ($\mathbf{X}$ being the position vector of $\mathbb{R}^3$). The instantaneous Lagrangian velocity $\mathbf{v}_\mathrm{L}$ of the vortex line at a point $\mathbf{X}$ is given by

$$\mathbf{v}_\mathrm{L} = \frac{\mathrm{d}\mathbf{X}}{\mathrm{d}t} = \mathbf{v}_\mathrm{self} + \alpha\hat{\mathbf{t}} \times (\mathbf{v}_\mathrm{n} - \mathbf{v}_\mathrm{self}), \tag{1}$$

where $\mathbf{v}_\mathrm{self} = \mathbf{v}_\mathrm{self}(\mathbf{X})$ is the self-induced velocity of the vortex $\mathcal{L}$, α a known temperature-dependent friction parameter, $\hat{\mathbf{t}} = \mathrm{d}\mathbf{X}/\mathrm{d}s$ the tangent unit vector to $\mathcal{L}$, and $\mathbf{v}_\mathrm{n}$ the super-imposed *ABC*-type normal fluid velocity [23,24] (we neglect a second, smaller, transverse friction parameter). During evolution, a tangle $\mathcal{T} = \bigcup_i \mathcal{L}_i$ of N vortex lines $\mathcal{L}_i$ $(i = 1, \ldots, N)$ develops. The motion of each vortex line in the fluid is dominated by the self-induced velocity $\mathbf{v}_\mathrm{self}$, given by the classical Biot–Savart integral

$$\mathbf{v}_\mathrm{self}(\mathbf{X}) = \frac{\Gamma}{4\pi}\int_{\mathcal{T}} \frac{(\mathbf{X}^* - \mathbf{X}) \times \hat{\mathbf{t}}}{|\mathbf{X}^* - \mathbf{X}|^3}\mathrm{d}s, \tag{2}$$

where $\mathbf{X}^*(s)$ varies along the lines and $\int_{\mathcal{T}} \cdot\, \mathrm{d}s$ denotes arc-length integration extended to the entire collection $\bigcup_i \mathcal{L}_i$ of vortex lines. The integral above is a global functional of the geometry and governs inviscid evolution. In the ideal case (Euler's equations), not only all the induction effects are retained, but also the topology of the vortex system is preserved (this is a property of the Euler's equations). In terms of numerical calculations, it is well known that the Biot–Savart integral diverges logarithmically as the field point approaches the source point on the filament. The classical method of overcoming this problem is to employ a cut-off by a standard procedure [1,2,23,24], which we shall follow and that is used extensively in literature [27,28]. This consists of de-singularising the integral by using a cut-off length δ (a measure of the aspect ratio of the vortex), substituting the singular part of the integral with the dynamics given by the leading-order approximation (the so-called localised induction approximation, LIA for short)

$$\mathbf{v}_\mathrm{LIA} = \frac{\Gamma}{4\pi R}(\ln\delta)\hat{\mathbf{b}}, \tag{3}$$

where $R = R(s) = |\mathrm{d}^2\mathbf{X}/\mathrm{d}s^2|^{-1}$ is the local radius of curvature and $\hat{\mathbf{b}}$ the binormal unit vector at $\mathbf{X}(s,t)$; δ is supposed to be finite as $\mathbf{X}^* \to \mathbf{X}(s,t)$ and is kept constant. The calculation of the vortex evolution is performed in an infinite box using a numerical technique that is described elsewhere [21,22].

Typical results of the generation and growth of a vortex tangle are shown in Fig. 2: the super-imposed *ABC* flow acts on a superfluid vortex ring (a: $t = 0\,\mathrm{s}$) generating disturbances that become unstable and develop Kelvin waves (b: $t = 0.015\,\mathrm{s}$). Since vortex dynamics is strongly influenced by curvature effects (see Eq. (3) above), the change in the initial vortex configuration determines a rapid growth in entanglement and interactions (c: $t = 0.050\,\mathrm{s}$); these trigger reconnections and a vortex tangle develops rapidly (d: $t = 0.087\,\mathrm{s}$).

Since the tangle $\mathcal{T}$ is the result of a numerical computation, its complexity can be analysed fairly easily by extracting information from available data. To do this efficiently, we make use of the concept of orthogonal projection p. Take the space curve $\mathcal{L}$ of Fig. 3

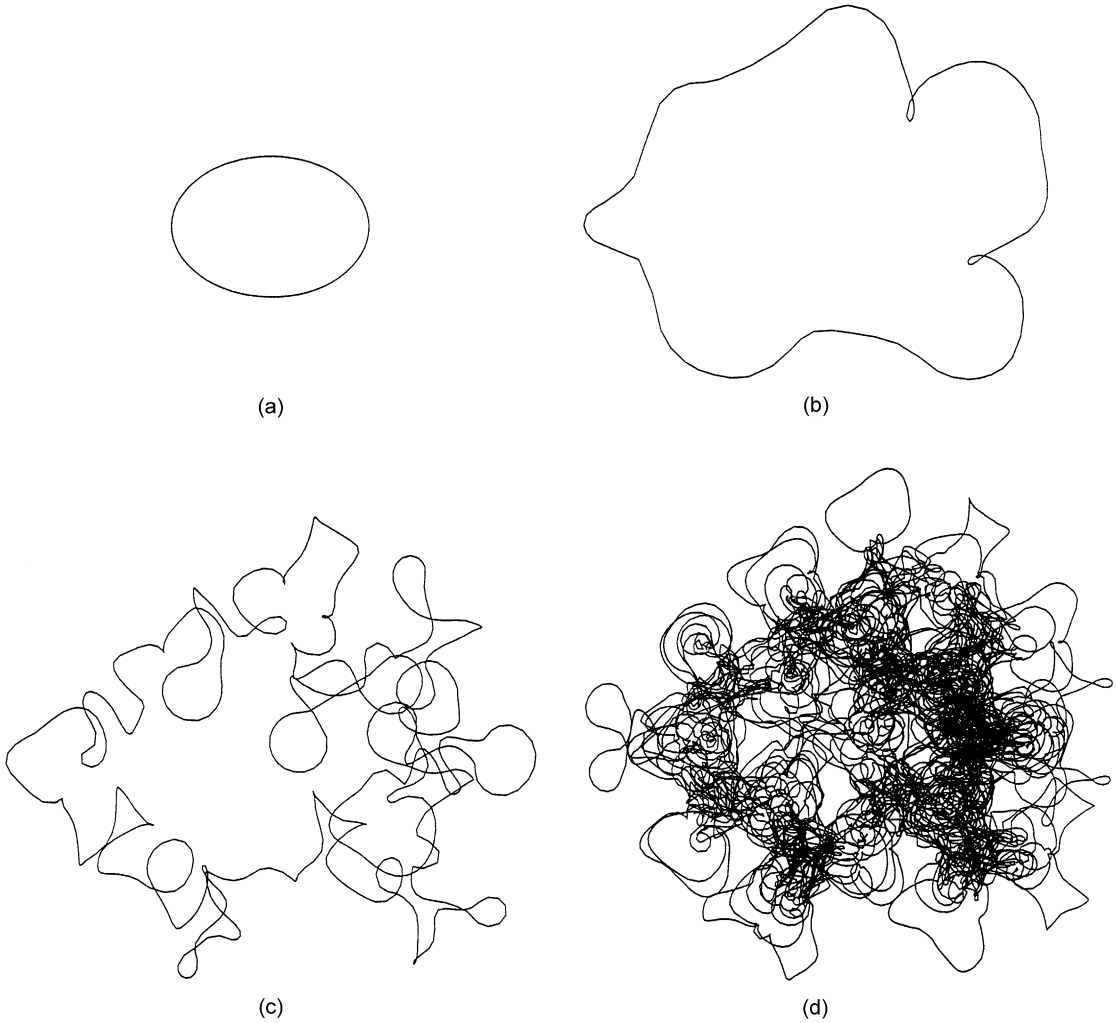

Fig. 2. Time sequence of the formation of a superfluid vortex tangle. All snapshots are plotted on the same scale. The super-imposed *ABC*-type normal flow acts (a: $t = 0\,\mathrm{s}$) on an initial seed vortex ring, (b: $t = 0.015\,\mathrm{s}$) producing instabilities that trigger reconnections; (c: $t = 0.050\,\mathrm{s}$) these produce further complexity and (d: $t = 0.087\,\mathrm{s}$) a vortex tangle is rapidly formed. The calculation is performed with $\alpha = 0.5$ and *ABC* flow parameters $A = B = C = 5\,\mathrm{cm/s}$, $\lambda = 1.0\,\mathrm{cm}$. The *ABC* flow [23,24] is defined as $\mathbf{v}_\mathrm{n} = [A\sin(2\pi z/\lambda) + C\cos(2\pi y/\lambda)]\hat{\mathbf{x}} + [B\sin(2\pi x/\lambda) + A\cos(2\pi z/\lambda)]\hat{\mathbf{y}} + [C\sin(2\pi y/\lambda) + B\cos(2\pi x/\lambda)]\hat{\mathbf{z}}$, where $\hat{\mathbf{x}}$, $\hat{\mathbf{y}}$ and $\hat{\mathbf{z}}$ are the unit vectors in the three cartesian coordinates x, y and z, respectively.

and project $\mathcal{L}$ orthogonally onto the plane Π_ν (say at $z = 0$) along the direction of projection $\boldsymbol{\nu}$: the projected curve $\mathcal{L}_\nu = p_\nu(\mathcal{L})$ is the projection diagram of $\mathcal{L}$ under p along $\boldsymbol{\nu}$ and it evidently depends on $\boldsymbol{\nu}$. The projected curve is a self-intersecting, planar curve, whose points of intersection correspond to the apparent crossings of $\mathcal{L}$, when it is seen along the line of sight $\boldsymbol{\nu}$. Self-intersections can be classified according to their degree of multiplicity given by the number of multiple points produced by the overlapping strands. A good projection, however, is given by a diagram whose graph has at most double points, which means that at each intersection no more than two strands cross transversally, being the intersection a point in isolation. By an appropriate choice of the projecting vector $\boldsymbol{\nu}$, we can always select good

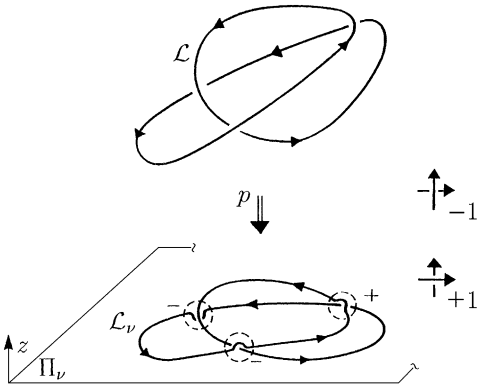

Fig. 3. An oriented, closed-vortex lines $\mathcal{L}$ is projected orthogonally under $p : \mathcal{L} \to \mathcal{L}_\nu$ onto the plane Π_ν (at $z = 0$). By allowing indentations into $z > 0$ or $z < 0$, we can assign the value $\epsilon_r = \pm 1$ to each intersection point of the oriented diagram according to the standard sign convention indicated.

projections; thus, we shall restrict the discussion below to good projections. If the curve $\mathcal{L}$ is oriented (being a vortex line the orientation of $\mathcal{L}$ is induced naturally by the prescribed vorticity), then $\mathcal{L}_\nu$ is also oriented and we can assign an algebraic value $\epsilon_r = \pm 1$ to each intersection point r of the oriented diagram according to standard convention, as shown in Fig. 3 [29]. By extending these concepts to a collection of N filaments $\mathcal{L}_i$ $(i = 1, \ldots, N)$, we can determine projection diagrams $\mathcal{T}_\nu$ by taking good projections of $\mathcal{T} = \bigcup_i \mathcal{L}_i$. We shall use these diagrams to compute complexity.

An algebraic measure of complexity is given by the *average crossing number* (see Freedman and He in [11–13]). For two loops $\mathcal{L}_i, \mathcal{L}_j$, this quantity is defined by

$$\bar{C}_{ij} = \frac{1}{4\pi} \oint_{\mathcal{L}_i} \oint_{\mathcal{L}_j} \frac{|(\mathbf{X}_i - \mathbf{X}_j) \cdot \mathrm{d}\mathbf{X}_i \times \mathrm{d}\mathbf{X}_j|}{|\mathbf{X}_i - \mathbf{X}_j|^3}, \tag{4}$$

where $\mathbf{X}_i \in \mathcal{L}_i$ and $\mathbf{X}_j \in \mathcal{L}_j$. A physical interpretation of this formula can be given by using the concept of solid angle. According to Moffatt and Ricca [30,31], suppose we view the curves $\mathcal{L}_i$ and $\mathcal{L}_j$ projected onto the plane Π_ν. We then see a number $r_+(\boldsymbol{\nu})$ of positive crossings and $r_-(\boldsymbol{\nu})$ of negative crossings. The elements $\mathrm{d}\mathbf{X}_i$, $\mathrm{d}\mathbf{X}_j$ intersect in projection if and only if $\boldsymbol{\nu}$ is parallel to $\pm(\boldsymbol{\rho} + \alpha\,\mathrm{d}\mathbf{X}_i - \beta\,\mathrm{d}\mathbf{X}_j)$, where $\boldsymbol{\rho} = \mathbf{X}_i - \mathbf{X}_j$ (see Fig. 4), $0 < \alpha < 1$ and $0 < \beta < 1$,

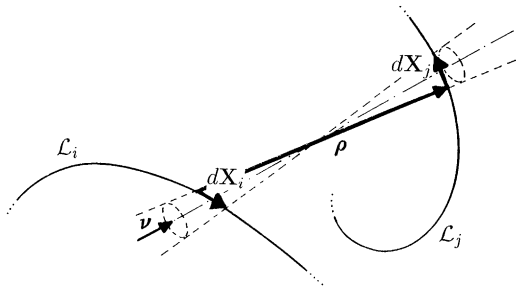

Fig. 4. Contribution to the solid angle by elements $\mathrm{d}\mathbf{X}_i$, $\mathrm{d}\mathbf{X}_j$ of $\mathcal{L}_i$ and $\mathcal{L}_j$, respectively. The $\boldsymbol{\nu}$-direction indicates a line of apparent intersection of $\mathrm{d}\mathbf{X}_i$ with $\mathrm{d}\mathbf{X}_j$.

i.e. only if $\boldsymbol{\nu}$ lies within a solid angle

$$\mathrm{d}\varpi = \frac{2(\mathrm{d}\mathbf{X}_i \times \mathrm{d}\mathbf{X}_j) \cdot \boldsymbol{\rho}}{4\pi\rho^3}, \tag{5}$$

where $\rho = |\boldsymbol{\rho}|$ (the factor 2 allowing for the $\pm$ possibilities above). Thus, when we average over all directions of $\boldsymbol{\nu}$, taking account of the absolute value and then integrating over all pairs of elements $\mathrm{d}\mathbf{X}_i$, $\mathrm{d}\mathbf{X}_j$, we obtain

$$\begin{aligned}\bar{C}_{ij} &= \frac{1}{4\pi} \oint_{\mathcal{L}_i} \oint_{\mathcal{L}_j} \frac{|\boldsymbol{\rho}| \cdot |\mathrm{d}\mathbf{X}_i \times \mathrm{d}\mathbf{X}_j|}{\rho^3} \\ &= \langle r_+(\boldsymbol{\nu}) + r_-(\boldsymbol{\nu}) \rangle,\end{aligned}$$

that is

$$\bar{C}_{ij} = \left\langle \sum_{r \in \mathcal{L}_i \cap \mathcal{L}_j} |\epsilon_r| \right\rangle, \tag{6}$$

where the angular brackets denote averaging over all directions $\boldsymbol{\nu}$ of projection. This gives an interpretation of (4) in terms of average number of apparent (and unsigned) crossings. This fact is evident from consideration of the diagram of Fig. 4. The natural generalisation of this measure to the entire collection of filaments gives

$$\bar{C} = \sum_{\mathcal{L}_i, \mathcal{L}_j \in \mathcal{T}} \bar{C}_{ij}. \tag{7}$$

Eq. (7) provides an algebraic measure of the complexity of $\mathcal{T}$, since it relates entanglement to apparent number of crossings. In the case of a very high density of vortex lines (hence of crossings), this measure

can be too expensive or even impossible to calculate; thus, it may be necessary to approximate $\bar{C}$ by taking an algebraic mean over a small number of projections in order to have an estimate of the average crossing number. Taking the three orthogonal, principal planes ($x = 0$, $y = 0$, $z = 0$) as projection planes, we define the *estimated average crossing number* as

$$\bar{C}_\perp = \left\langle \sum_{r\in\mathcal{I}_v} |\epsilon_r| \right\rangle_\perp , \tag{8}$$

where $\langle\cdot\rangle_\perp$ indicates that the solid angle average is replaced by the algebraic mean over the three principal planes of projection.

Geometric quantities such as total length $L = \int_{\mathcal{T}} \mathrm{d}s$ of the tangle and total curvature may also provide useful information to classify complex patterns. An interesting quantity is the writhing number Wr. For a single filament we have $Wr_i = Wr(\mathcal{L}_i)$, defined by

$$Wr_i = \frac{1}{4\pi} \oint_{\mathcal{L}_i} \oint_{\mathcal{L}_i} \frac{(\mathbf{X}_i - \mathbf{X}_i^*)\cdot \mathrm{d}\mathbf{X}_i \times \mathrm{d}\mathbf{X}_i^*}{|\mathbf{X}_i - \mathbf{X}_i^*|^3}, \tag{9}$$

where $\mathbf{X}_i$ and $\mathbf{X}_i^*$ are now two points of the same filament $\mathcal{L}_i$ and integration is performed twice on the same curve. By using geometric and topological arguments [30,31], it is possible to show that the writhing number provides actually a global geometric measure of the average total coiling of $\mathcal{L}_i$ in space; in other words, it provides a measure of the amount of curvature in a given configuration. By the same solid angle argument used for the integrand of Eq. (4), we can show that

$$Wr_i = \langle r_+(\boldsymbol{\nu}) - r_-(\boldsymbol{\nu})\rangle = \left\langle \sum_{r\in\mathcal{L}_i\cap\mathcal{L}_i} \epsilon_r \right\rangle, \tag{10}$$

where now the average is extended to the number r of apparent, *signed* crossings (self-intersections) of $\mathcal{L}_i$ seen along the line of sight $\boldsymbol{\nu}$ (note the minus sign in front of $r_-(\boldsymbol{\nu})$). A measure of the geometric complexity of the whole tangle is provided by the average total coiling of $\mathcal{T}$ given by averaging the crossing number measure over the whole collection of filaments, hence

$$Wr = Wr(\mathcal{T}) = \left\langle \sum_{r\in\mathcal{T}} \epsilon_r \right\rangle. \tag{11}$$

As above, it may be computationally convenient to approximate Wr by the *estimated writhing number* $Wr_\perp$, given by

$$Wr_\perp = \left\langle \sum_{r\in\mathcal{T}_v} \epsilon_r \right\rangle_\perp . \tag{12}$$

A useful concept for a topological measure of complexity is provided by the linking coefficient Lk [29]. The linking number $Lk_{ij} = Lk(\mathcal{L}_i, \mathcal{L}_j)$ between two closed loops $\mathcal{L}_i$ and $\mathcal{L}_j$ is defined by the Gauss formula, which is formally identical to Eq. (4), with the exception of the absolute value sign at the numerator of the integrand. It is well known that Lk_{ij} provides a measure of the topological linking between closed, linked curves and admits interpretation in terms of minimal number of crossings. In terms of crossing number, it can be defined by the formula

$$Lk_{ij} = \frac{1}{2} \sum_{r\in\mathcal{L}_i\cap\mathcal{L}_j} \epsilon_r . \tag{13}$$

The linking number Lk_{ij} is one of the most fundamental topological invariants of link types. This means that it does not change under continuous deformations of the vortex strands (i.e. under Reidemeister moves performed on the vortex strands, cf. [29–31]), that conserve the topology but not the geometry. In terms of numerical calculations, this means that the linking number does not change value under a change of projection plane (since p is a continuous function of $\boldsymbol{\nu}$ and a continuous change in projection corresponds to a continuous change in the projected geometry); hence, we can calculate Lk_{ij} on the projected geometry of our choice, its value remaining unchanged as long as reconnections do not take place. The *total linking* Lk_{tot} of a system of vortex lines can be defined by

$$Lk_{\mathrm{tot}} = \sum_{\substack{\mathcal{L}_i,\mathcal{L}_j\in\mathcal{T} \\ i\neq j}} |Lk_{ij}|, \tag{14}$$

where we deliberately exclude contributions from self-linking (due to writhe and twist of each vortex filament; see [30,31]). Lk_{tot} provides a measure of topological complexity of the system.

Another quantity that relates topology of the system to the physics is the *kinetic helicity* [32], defined by

$$H = \int_V \mathbf{v}_\mathrm{L} \cdot \boldsymbol{\omega} \, \mathrm{d}^3\mathbf{X}, \tag{15}$$

where $\boldsymbol{\omega}$ is the vorticity and the integral is taken over the tangle volume $V = V(\mathcal{T})$. Since vorticity is confined only to vortex lines, $\boldsymbol{\omega}$ is a delta function of strength Γ in the direction $\hat{\mathbf{t}}$ along each filament of $\mathcal{T}$, so, we have

$$H = \Gamma \int_{\mathcal{T}} \mathbf{v}_\mathrm{L} \cdot \hat{\mathbf{t}} \, \mathrm{d}s, \tag{16}$$

where $\mathbf{v}_\mathrm{L}$ is the velocity of the filament (not to be confused with the fluid velocity around the filament), and, as for Eq. (2), the line integral is extended to the whole tangle of vortex lines. Helicity is a measure of the total linking between $\mathbf{v}_\mathrm{L}$-lines and vortex lines. It can be related to the linking (via the Gauss linking number) and the self-linking (via the so-called Călugăreanu–White invariant [30,31]) of vortex filaments, but in this paper we shall not make use of this relationship. We shall calculate helicity simply by using Eq. (16) above, that provides a direct measure and an alternative means for comparison with the other results.

All these measures are then compared against the kinetic energy E of the system, which is ultimately the most important physical information. For the vortex tangle we have

$$E = \frac{\rho_\mathrm{s}}{2} \int_V v^2 \, \mathrm{d}^3\mathbf{X}, \tag{17}$$

where $\mathbf{v}$ is the Eulerian superfluid velocity, $v^2 = \mathbf{v} \cdot \mathbf{v}$ and ρ_s the superfluid density. It is not practical to use (17) directly to calculate the energy of a tangle of vortex filaments due to the discretization errors caused by the rapidly changing velocity field $\mathbf{v}$ in the vicinity of a vortex filament. It is better to proceed using the following formula of Lamb [25,26] which we rederive in Appendix A for the sake of completeness:

$$\frac{1}{2} \int_V v^2 \, \mathrm{d}^3\mathbf{X} = \int_V \mathbf{v} \cdot (\mathbf{X} \times \boldsymbol{\omega}) \, \mathrm{d}^3\mathbf{X}. \tag{18}$$

Since the vorticity is concentrated along filaments, the integral can be reduced to a line integral (as for the helicity) and from (17) and (18), we conclude that the energy is

$$E = \frac{\rho_\mathrm{s}\Gamma}{2} \int_{\mathcal{T}} \mathbf{v} \cdot \mathbf{X} \times \hat{\mathbf{t}} \, \mathrm{d}s. \tag{19}$$

3. Discussion of results and conclusions

As the tangle develops, we calculate average crossing numbers, writhing numbers and total linking as well as total length, kinetic helicity and energy. The results of the calculations are plotted against time and are shown in Fig. 5. In order to compare growth rates, we plot all the quantities on a linear-log scale. Length and energy are normalised with respect to their initial values (respectively, L_0 and E_0), and in order to plot helicity on the same diagram with the other quantities, we re-scale helicity with a constant. At time $t = 0$, only a single vortex ring is present and complexity is evidently zero. As the vortex structure unfolds, the dynamics develops complexity and entanglement. Since both average crossing number and writhing number depend on the actual space configuration of the filaments, their values change continuously as the tangle changes shape and evolves in time. The initial growth of length is in agreement with linear stability calculations [23,24], and the (expected) marked similarity of energy and length growth rates confirms the importance of monitoring length (directly measured in the experiments) as a measure of the energy of the system.

We can approximately identify two stages of evolution, that we ideally separate by the first occurrence of a reconnection event. In the first stage, the initial seed vortex ring (with $Lk_\mathrm{tot} = 0$) develops a geometrically complex structure, but no entanglement; throughout this stage reconnections do not take place and the topology of the vortex pattern remains unchanged: thus, Lk_tot remains zero. The first reconnection takes place at the first non-zero value of total linking Lk_tot at $t \approx 0.06$ s (at about 2 on the y-axis). This can be taken as a marker for the beginning of the second stage of evolution (which we may identify with mature growth), in which entanglement and topological changes do take place. For $t > 0.06$ s, the growth rates of $Wr_\perp$, $|H|$, $\bar{C}_\perp$ and $\bar{C}$ (respectively,

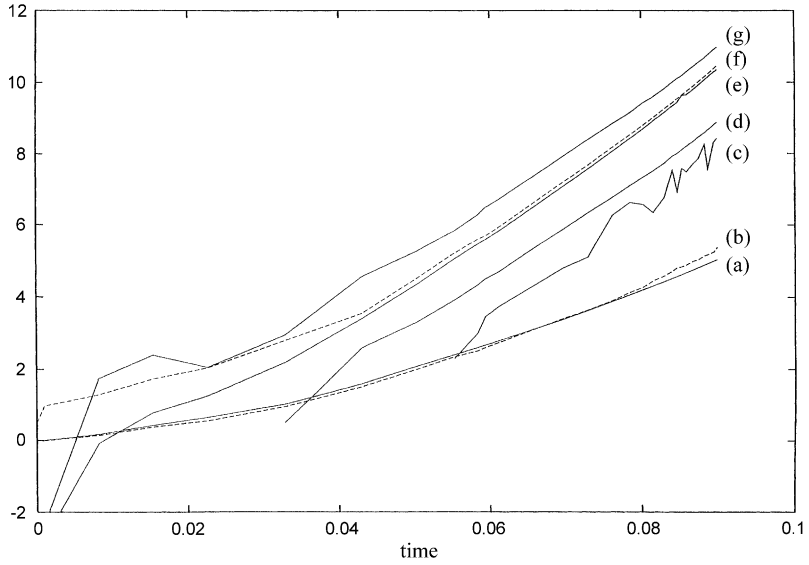

Fig. 5. Measures of complexity, helicity and energy in logarithmic scale versus time: (a) length $\ln(L/L_0)$; (b) energy $\ln(E/E_0)$; (c) total linking $\ln(Lk_{\rm tot})$; (d) estimated writhing number $\ln(Wr_\perp)$; (e) average crossing number $\ln(\bar{C})$; (f) estimated average crossing number $\ln(\bar{C}_\perp)$; (g) absolute helicity $\ln(|H|)$. For $t > 0.06\,$s, the tangle is in a mature growth stage and complexity is well identified by the marked similarity of the growth rates of algebraic, geometric and topological measures.

152.2, 153.6, 164.7 and 166.2 $\rm s^{-1}$) show remarkable similarities, being all about twice the growth rates of energy and length (82.8 $\rm s^{-1}$).

It is noteworthy that there is a factor of approximately 2 between the growth rates of energy and complexity measures, $E \sim \mathcal{X}^2$. This relation apparently arises because the tangle grows in length by curling up and folding upon itself more than by spreading out and diffusing in space. Consider a collection of N segments of equal length which are put on top of each other on a plane. If a segment is added over the existing segments, the number of crossings $K = K(N)$ becomes $K(N+1) = K(N) + N$ since the new segment will cross at the most all the existing N segments. Hence $K = \frac{1}{2}(N^2 - N)$, i.e. to say $K \sim N^2$. If we have a continuum, then the number of new crossing per unit length of added line is proportional to the existing line length, $\mathrm{d}K/\mathrm{d}L \sim L$, hence $K \sim L^2$. This simple model is relevant to the tangle, because all complexity measures are consistent with the average crossing number which can be interpreted in terms of apparent crossings projected against the solid sphere. In fact we find that the length L, which is a good measure of the energy E, grows such that $\bar{C} \sim L^2$, in agreement with $K \sim N^2$. Physically, this result means that there is little diffusion of vortex lines away from the tangle. Why it should be so is a problem of superfluid hydrodynamics which clearly deserves a detailed investigation. Here we simply note that small vortex rings of size less than the average intervortex spacing occasionally escape from the tangle, but these events are relatively uncommon and do not contribute significantly to the tangle's diffusion outward in space. The length's growth process is via destabilisation of helical Kelvin waves, hence the apparent folding of the tangle upon itself.

The almost identical behaviour of $\bar{C}_\perp$ and $\bar{C}$ (less than 1% difference in growth rate) confirms the conjecture (of RLR) that $\bar{C}_\perp$ provides indeed a good approximation for algebraic measure of structural complexity. As evidenced by the larger deviation present at earlier times, this approximation get worse when the number of crossings is low. Another interesting feature is represented by the marked similarity of the growth rates of $|H|$ and $Wr_\perp$ (also less than 1% difference), showing that the change in geometric

coiling measured by $Wr_\perp$ follows closely the variation in topological complexity of the tangle. Moreover, the fact that the growth rates of $|H|$ and $\bar{C}$ differ only by about 8% shows also the important role of helicity in capturing the morphological complexity of disordered system. The marked fluctuations of $Lk_{\rm tot}$ are simply due to reconnection events, which determine the computation of the topological linking of the system, that does not change until a reconnection takes place. Numerical tests show that these fluctuations become smaller as the tangle becomes denser (i.e. as L increases). Still, it is noteworthy that the numerical fit estimate of $Lk_{\rm tot}$ gives a growth rate of $173.0\,{\rm s}^{-1}$, i.e. only about 12% different from the other rates.

In conclusion, we have identified superfluid vortex tangle simulations as convenient numerical benchmarks to study the complexity of physical systems in the presence of filamentary structures. The vortex tangle has been produced by super-imposing an *ABC*-type of flow to simulate the action of a localised eddy. One motivation behind the use of an *ABC* flow is to make contact with previous work in the helium literature [23,24]. The *ABC* flow is highly helical. The initial stage of growth is fast [23,24] and has the advantage of maximising the input of helicity and entanglement: while the effects of this flow are to enhance topological linking (by a selective production of disturbances), the comparative relationship between growth rates has generic characteristics. We have introduced and tested various measures of algebraic, geometric and topological complexity in an actual turbulence problem, i.e. the growth of a superfluid tangle driven by a normal fluid eddy. We have computed these measures as the tangle evolves and found marked similarities in their growth rates. The agreement proves that all these measures (and in particular average crossing number measures and helicity) are good markers for complexity. Moreover, the growth rate for complexity (and in particular that for helicity) is much larger than the growth rate of length and energy. This is also an interesting result that merits further investigation. From a numerical viewpoint, we notice that the computation of quantities like $\bar{C}_\perp$ is numerically robust and more robust than the integration required to determine $\bar{C}$. Since the growth rates of these two quantities are so close (<1%), we prove that it is approximately correct to use $\bar{C}_\perp$ in general computational methods to keep track of structural complexity and hence identify patterns in disordered systems. The techniques which we use are of general interest and can be applied to study many other physical and biological problems.

Acknowledgements

RLR acknowledges the financial support of EPSRC (grant GR/K99015).

Appendix A

For the sake of completeness, here we rederive Lamb's formula (18). We start by remarking that $\mathbf{v}\cdot(\mathbf{X}\times\boldsymbol{\omega}) = -\mathbf{X}\cdot(\mathbf{v}\times\boldsymbol{\omega}) = \mathbf{X}\cdot[(\mathbf{v}\cdot\nabla)\mathbf{v}] - \mathbf{X}\cdot\nabla(\frac{1}{2}v^2) = (\mathbf{v}\cdot\nabla)(\mathbf{v}\cdot\mathbf{X}) - \mathbf{v}\cdot[(\mathbf{v}\cdot\nabla)\mathbf{X}] - \nabla\cdot(\frac{1}{2}v^2\mathbf{X}) + \frac{1}{2}v^2(\nabla\cdot\mathbf{X})$.

Since $\nabla\cdot\mathbf{X} = 3$, $\nabla\cdot\mathbf{v} = 0$ and $(\mathbf{v}\cdot\nabla)\mathbf{X} = \mathbf{v}$, we have $\mathbf{v}\cdot(\mathbf{X}\times\boldsymbol{\omega}) = \frac{1}{2}v^2 + \nabla\cdot[\mathbf{v}(\mathbf{v}\cdot\mathbf{X}) + \frac{1}{2}v^2\mathbf{X}]$. Integrating the equation over the volume V and using the Divergence theorem, we obtain

$$\int_V \frac{v^2}{2}\,{\rm d}^3\mathbf{X} = \int_V \mathbf{v}\cdot(\mathbf{X}\times\boldsymbol{\omega})\,{\rm d}^3\mathbf{X} - \int_S \left[(\mathbf{v}\cdot\hat{\mathbf{n}})(\mathbf{v}\cdot\mathbf{X}) + \frac{v^2}{2}(\mathbf{X}\cdot\hat{\mathbf{n}})\right]{\rm d}S,$$

where S is the surface bounding V and $\hat{\mathbf{n}}$ the unit vector in the normal direction out of S. If the fluid is unbound, the surface integral vanishes at infinity and we recover Lamb's formula (18):

$$\frac{1}{2}\int_V v^2\,{\rm d}^3\mathbf{X} = \int_V \mathbf{v}\cdot(\mathbf{X}\times\boldsymbol{\omega})\,{\rm d}^3\mathbf{X}.$$

References

[1] K.W. Schwarz, Phys. Rev. B 31 (1985) 5782.
[2] C.F. Barenghi, J. Phys. 11 (1999) 7751.
[3] H.C. Spruit, B. Roberts, Nature 304 (1983) 401.
[4] P.G. De Gennes, Introduction to Polymer Dynamics, Lezioni Lincee, Cambridge University Press, Cambridge, 1990.
[5] A. Vologodskii, N. Crisona, B. Laurie, P. Pieranski, V. Katritch, J. Dubochet, A. Stasiak, J. Mol. Biol. 278 (1998) 1.
[6] B. Allen, E.P.S. Shellard, Phys. Rev. Lett. 64 (1990) 119.

[7] R.L. Ricca, M.A. Berger, Phys. Today 49 (12) (1996) 24.
[8] R.L. Ricca, in: C.McA. Gordon, et al. (Eds.), Knots in Hellas'98, Series on Knots and Everything, Vol. 24, World Scientific, Singapore, 2000, p. 361.
[9] K.C. Millett, D.W. Sumners (Eds.), Random Knotting and Linking, Series on Knots and Everything, World Scientific, Singapore, 1994, p. 7.
[10] R.W. Ghrist, P.J. Holmes, M.C. Sullivan, Knots and links in three-dimensional flows, Lecture Notes in Mathematics, Springer, Berlin, 1997, p. 1654.
[11] H.K. Moffatt, Nature 347 (1990) 367.
[12] M.H. Freedman, Z.-X. He, Ann. Math. 134 (1991) 189.
[13] M.A. Berger, Phys. Rev. Lett. 70 (1993) 705.
[14] R.J. Donnelly, Quantized Vortices in Helium II, Cambridge University Press, Cambridge, 1991.
[15] W.F. Vinen, Phys. Rev. B 61 (2000) 1410.
[16] J. Koplik, H. Levine, Phys. Rev. Lett. 71 (1993) 1375.
[17] P.L. Walstrom, J.G. Weisend, J.R. Maddocks, S.V. VanSciver, Cryogenics 28 (1988) 101.
[18] J. Maurer, P. Tabeling, Europhys. Lett. 43 (1998) 29.
[19] S.R. Stalp, L. Skrbek, R.J. Donnelly, Phys. Rev. Lett. 82 (1999) 4381.
[20] P.C. Hendry, N.S. Lawson, P.V.E. McClintock, J. Low Temp. Phys. 119 (2000) 249.
[21] D.C. Samuels, Phys. Rev. B 46 (1992) 11714.
[22] M. Tsubota, T. Araki, S.K. Nemirowskii, J. Low Temp. Phys. 119 (2000) 337.
[23] D.C. Samuels, Phys. Rev. B 47 (1993) 1107.
[24] C.F. Barenghi, G. Bauer, D.C. Samuels, R.J. Donnelly, Phys. Fluids 9 (1997) 2631.
[25] H. Lamb, Hydrodynamics, 6th Edition, Cambridge University Press, Cambridge, 1932.
[26] P.G. Saffman, Vortex Dynamics, Cambridge University Press, Cambridge, 1992.
[27] A. Leonard, J. Comput. Phys. 37 (1980) 239.
[28] P. Moin, A. Leonard, J. Kim, Phys. Fluids 29 (1986) 955.
[29] L.H. Kauffman, On Knots, Annals Study, Princeton University Press, Princeton, NJ, 1987, p. 115.
[30] H.K. Moffatt, R.L. Ricca, Proc. R. Soc. London A 439 (1992) 411.
[31] R.L. Ricca, in: V.F.R. Jones, et al. (Eds.), Knot Theory, Vol. 42, Banach Center Publications, Polish Academy of Sciences, Warsaw, 1998, p. 321.
[32] H.K. Moffatt, J. Fluid Mech. 35 (1969) 117.